RSC Advances




ROYAL SOCIETY OF CHEMISTRY

www.rsc.org/advances

# Sandwich composites of polyurethane reinforced with poly (3, 4-ethylene dioxythiophene) coated multiwalled carbon nanotubes with exceptional electromagnetic interference shielding properties

**M. Farukh[ab], Ridham Dhawan[a], Bhanu P. Singh[c] and S.K.Dhawan[a*]**

[a] Polymeric & Soft Materials Section, CSIR-National Physical Laboratory, Dr. K. S. Krishnan Road, New Delhi –110 012 (India)

[b]Academy of Scientific and Innovation Research, CSIR-National Physical Laboratory, Dr. K. S. Krishnan Road, New Delhi –110 012 (India)

[c] Physics and Engineering of Carbon, Division of Materials Physics and Engineering, CSIR-National Physical Laboratory, New Delhi, 110012 (India)

---

** Corresponding author. Tel.: +91-11-45609401, Fax: +91-11-25726938*

*E-mail address: skdhawan@mail.nplindia.org*

**Abstract:** Poly (3, 4-ethylene dioxythiophene) (PEDOT) coated multiwalled carbon nanotube (MWCNT) composite (PCNT) was synthesized by in-situ emulsion polymerization and was used as a filler for fabrication of polyurethane (PU) sandwich composites (PUPCNT) by solution casting technique. Transmission electron microscopy (TEM) images revealed coating of PEDOT over MWCNT and the scanning electron microscopy (SEM) micrographs show uniform dispersion of PCNT filler in the fractured surface analysis of PUPCNT films which was further confirmed by X-ray diffraction (XRD) analysis. The tensile strength of all the PUPCNT composites indicated that tensile strength do not degrade on adding 10 and 20 % PCNT filler in the PU matrix. Electrostatic charge dissipation (ESD) measurements of PEDOT filled PU composites shows a static decay time of 0.2 sec which can be utilized for antistatic applications. The PUPCNT composites showed excellent electromagnetic interference shielding effectiveness (EMI SE) which increases with the increase in filler loading in the PU matrix. The maximum EMI SE obtained was 45 dB with 30 wt% loading of PCNT filler in the frequency range of 12.4-18 GHz (Ku-band).

## 1. Introduction

With the development of Hi-tech systems, there has been an increase in the use of electronic and electrical equipments, which radiate and are affected by electromagnetic (EM) waves by a phenomenon called electromagnetic interference (EMI). Thus, shielding of both electronic instruments and radiation source is essential to maintain their functionality and integrity for a longer span of time. Conventional materials that were mainly used for EMI shielding purpose include metals and metallic composites[1-4]. However, these materials are associated with several disadvantages such as heavy weight, easy corrosion and expensive processing techniques. On the other hand, extrinsically conductive polymer composites and intrinsically conducting polymer (ICP) composites with various conducting fillers offer [1]superior properties over metal based shielding materials. They are light weight, anti-corrosive, flexible, and have processing advantages[5-6]. The EMI shielding effectiveness of a composite depends on the intrinsic conductivity, high aspect ratio and dispersion state of the conducting filler in the polymer matrix. ICPs represents a novel class of materials useful for EMI shielding[6] applications. They possess π-conjugated system which provides conductivity to the polymer. PEDOT, a derivative of polythiophene, represents a new member of conducting polymer family. It possess excellent environmental stability, low redox potential, good thermal stability, ease to synthesis with moderately high conductivity and is widely used for electro-chromic devices, organic solar cells, light emitting diodes and anti-static applications[7-10].

Conducting polymer grafted carbon nanotube (CNT) composites[11-13] can be considered as a useful approach for the fabrication of EMI shielding materials. CNTs are advanced fillers for improving the physical properties of polymers due to their excellent electrical and thermal conductivity, high aspect ratio, high mechanical strength, which makes them perfect candidate for the preparation of electrically conductive polymer composites. But the major obstruction in the use of CNTs as a reinforcement in the polymer matrix is their uneven dispersion in the matrix due to strong interfacial adhesion resulting in high tendency to agglomerate. However, the development of efficient processes and chemical treatment methods have solve these problems to some extent, but they might result in deterioration of properties of CNTs. There are numerous efforts been made by researchers to develop electrically conductive polymer composites using CNTs as filler for EMI shielding applications. Recently, Junye Cheng et al. synthesized polyaniline grafted CNT composite by pre-treating CNTs with plasma and then coated CNT with polyaniline by in-situ

polymerization. The maximum reflection loss observed was 41.37 dB for 2 mm thickness in the frequency range of 2-18 GHz[14]. Kotsilkova *et al* studied EMI shielding properties of amine grafted-MWCNTs/epoxy composites at very low wt% loading of MWCNTs (0.3 wt%) and observed EMI SE of 17 dB at 1 cm thickness[15]. Mohammed Al Saleh prepared composite by placing CNTs at the external surface of the ultrahigh molecular weight polyethylene powder by wet mixing and found EMI shielding effectiveness of 50 dB for a 1.0 mm thick plate made with 10% CNT loading[16]. Verma *et al* blended MWCNT (4.6 vol.%) in the polypropylene random copolymer using twin-screw extruder with melt re-circulator and reported an EMI shielding of 47 dB in the X-band [17]. Chen *et al* successfully prepared flexible and conductive materials using quartz fibre cloth reinforced MWCNT-carbon aerogel and polydimethyl siloxane, the composite exhibits increased tensile strength and EMI shielding of 16 dB at very low MWCNTs (1.6 wt%) loading[18]. Gupta *et al* reported fabrication of acid modified MWCNTs reinforced PU composites by solution casting[19] and observed EMI SE of ~29 dB with 10 wt% loading of MWCNTs in the X-band. Hoang dispersed MWCNTs in the PU matrix by grinding them in a planetary ball mill and an EMI SE of 20 dB was observed with 22 wt% MWCNTs in a frequency range of 8-12 GHz[20]. Ramoa et. al. prepared thermoplastic PU/CNTs composites through melt blending and investigated their EMI SE as a function of filler loading[21]. They reported maximum EMI SE of 22 dB in the frequency range of 8-12 GHz. Battacharya et. al. investigated microwave absorption properties of thermoplastic PU incorporated with $TiO_2$ coated MWCNTs (15%) and magnetite $Fe_2O_3$ (15%) by solution blending and showed maximum reflection loss of 42.53 dB at 10.98 GHz frequency[22]. A detailed comparison of various polymer composites prepared for EMI shielding applications containing CNTs as filler is given in table 3.

To unfold the processing problem of pristine CNTs and to explore combined effect of MWCNTs and conducting polymer PEDOT, we have synthesized PEDOT coated MWCNTs composite (PCNT). The combination of good dispersion properties of dodecylbenzene sulfonic acid (DBSA) doped PEDOT in many organic solvents and excellent electrical conductivity and mechanical properties of MWCNTs, results in the formation of unique PCNT composite with high processability, superior mechanical and electrical conductivity. In order to find the practical application of PCNT composite, we have fabricated PCNT composite into PU matrix as filler by simple solution casting for EMI shielding application. PU is known for its unique properties like good elasticity, high impact strength and elongation. These properties make PU a suitable candidate for the fabrication of flexible free

standing films. The DBSA doped PEDOT imparts high dispersibility in the processing medium and prevents agglomeration of MWCNTs resulting in the formation of uniformly distributed PCNT in the PU matrix.

EMI shielding effectiveness of resulting free standing PUPCNT films have been measured in the frequency range of 12.4-18 GHz (Ku-band). The value of EMI SE increases remarkably with increasing wt% of PCNT in the PU matrix. This can be attributed to the enhanced conductive network formed due to uniform dispersion of PCNT in the PU matrix. To the best of our knowledge, no studies have been reported so far on the fabrication of PEDOT coated MWCNTs as filler in PU for EMI shielding applications.

## 2. Materials

The monomer 3, 4-ethylene dioxythiophene (EDOT) was procured from TCI Chemicals, Japan. DBSA was purchased from Acros Organics (Belgium). Ammonium peroxydisulphate (APS) was procured from Merck (India). Isopropyl alcohol (IPA) and N, N-dimethyl formamide (DMF) were obtained from Qualigens (India). Thermoplastic PU (Desmopan 385 S) was procured from Bayer (India). The MWCNTs were synthesized by chemical vapour deposition (CVD) technique using toluene as carbon source and ferrocene as catalyst precursor. The as produced MWCNTs were 90% pure with diameter range between 20-50 nm and length between 50-100 μm[23].

## 3. Method

### 3.1 Synthesis of PEDOT

The PEDOT was synthesized by oxidative emulsion polymerization of EDOT using DBSA and APS as dopant and oxidant, respectively. In this method, 0.1 M EDOT and 0.3 M DBSA were emulsified in an aqueous medium at room temperature for an hour. The polymerization was initiated by addition of 0.1 M of APS solution drop-wise to the EDOT emulsion with constant stirring at −2 ℃. After 12 hours of stirring bluish black precipitate of PEDOT was obtained and demulsified with IPA under vigorous stirring. After demulsification, the precipitate was washed with distilled water, filtered and dried in vacuum oven for 24 hrs at 60 ºC.

### 3.2 Synthesis of PCNT

The encapsulation of MWCNTs in the PEDOT was carried out by in-situ polymerization. The MWCNTs was taken with respect to weight of EDOT in ratio (1 EDOT: 0.25 MWCNT) in 0.3 M aqueous DBSA solution and homogenized at 12000 rpm for 2 hours. The 0.1 M EDOT was then added to the above solution and stirred for 2 hours, after that 0.1 M APS was added drop-wise to this solution with continuous stirring at temperature $-2$ ℃. The PCNT composite obtained after 12 hrs of continuous stirring was treated with IPA for demulsification. The resulting precipitate was filtered, washed with distilled water and then dried in vacuum oven for 24 hours at 60 ℃.

### 3.3 Fabrication of PUP and PUPCNT composite films

The PUP (polyurethane incorporated with PEDOT) and PUPCNT composite films were prepared by simple solution casting method. The compounding formulation of composite with different wt % loading of PEDOT and PCNT as fillers is given in table 1. The schematic for the preparation of PUPCNT composite is depicted in Fig 1. Initially, PU granules were dissolved in DMF at 40 ℃ for 8 hours on the other hand PEDOT/PCNT filler was dispersed in another beaker in DMF under ultra-sonication for an hour. The dispersed PEDOT/PCNT filler in DMF and dissolved PU in DMF were mixed thoroughly for 2 hours. The mixed solution was then poured into a petri-dish and then kept for oven drying at 60 ℃ for 12 hours.

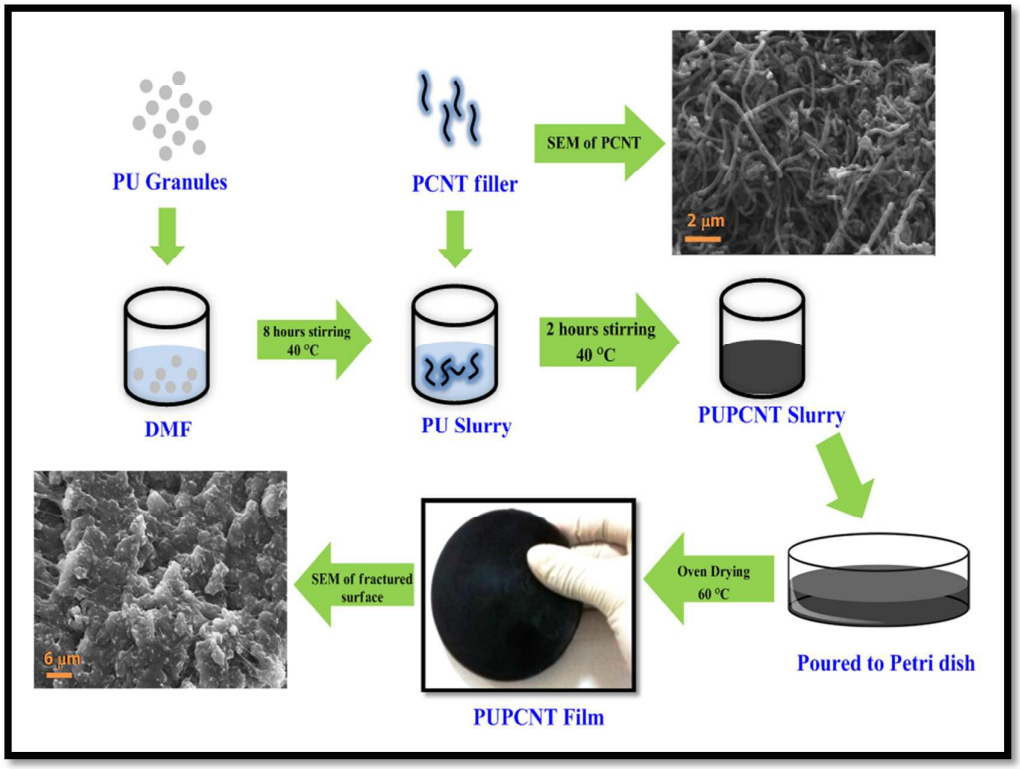

**Fig 1** Process for fabrication of PUPCNT composite film by solution casting

**Table 1** Compounding Formulations of composites containing different wt% loading of PEDOT/PCNT filler in PU matrix

| Sl No. | Sample | PU | PEDOT | PCNT* |
|---|---|---|---|---|
| 1. | PU | 100% | 0 | 0 |
| 2. | PUP1 | 90% | 10% | 0 |
| 3. | PUP2 | 80% | 20% | 0 |
| 4. | PUP3 | 0 | 30% | 0 |
| 5. | PUPCNT1 | 90% | 0 | 10% |
| 6. | PUPCNT2 | 80% | 0 | 20% |
| 7. | PUPCNT3 | 70% | 0 | 30% |

PCNT*: PEDOT coated MWCNTs (EDOT to MWCNT ratio was 1:0.25)

## 4. Material Characterization

The morphological analyses were carried out by SEM (Zeiss EVO MA-10) at an accelerating voltage of 10kV and TEM (Technai G20-stwin, 300 kV instrument). XRD measurements were carried out by D8 Advance XRD (Bruker) using Cu K-α radiation (λ=1.54 A◦) at the scanning rate of 0.02 °/sec and slit width of 0.1 mm. Fourier Transform Infrared (FTIR) spectra was recorded on a Nicolet 5700 using ATR (attenuated total reflectance) accessory. Tensile strength was measured with an ASTM D3039 dog bone die using Instron Universal Testing Machine (model 1122) at the rate of 2 mm/minute. The electrical conductivity of the composite films was measured by two probe technique using Keithley current source (model 6221) and nano-voltmeter (model 2182 A) at room temperature. Electrostatic dissipation measurements were carried out using JCI 155v5 charge decay test unit. Electromagnetic shielding measurements were carried out using Agilent E8362B Vector Network Analyzer having coaxial cable attached with rectangular waveguide of Ku-band (15.75 mm x 7.85 mm). The samples were cut into rectangular pellets of standard Ku-band dimensions and the thickness of the samples was kept ~2.5 mm.

## 5. Results and discussion

### 5.1 Morphological Analysis

The morphology and distribution of MWCNTs in the PU matrix were analysed with the help of SEM and TEM. Fig 2 (a) show the SEM micrograph of individual MWCNTs after dispersion in DMF, prepared over silicon wafer. It can be observed that MWCNTs are snarled to each other but some individual MWCNTs are easily distinguishable. Fig 2 (b) shows the granular/particulate amorphous nature of PEDOT which is further confirmed by XRD (see Fig 5). Fig 2 (c) and (d) show SEM images of PCNT filler at low and high magnifications, respectively. The PCNT presents a homogenous structure and look like rods of snowflakes. The nano-sized MWCNTs having high surface area serves as a nucleation sites for polymerization of EDOT monomer to form coating over MWCNTs. The images show uniform coating of the PEDOT over MWCNTs thereby forming high aspect ratio filler, responsible for good electrical conductivity of PUPCNT composites.

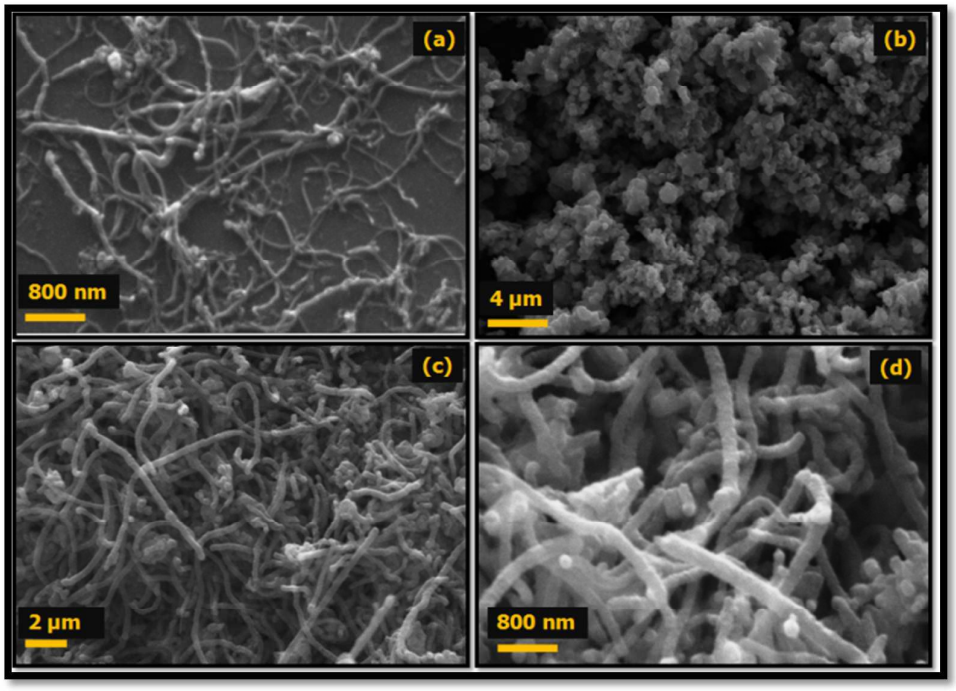


**Fig 2** SEM micrographs of (a) MWCNTs, (b) pure PEDOT polymer, (c) & (d) low and high magnification images of PCNT filler showing uniformly grafted PEDOT over MWCNTs, respectively

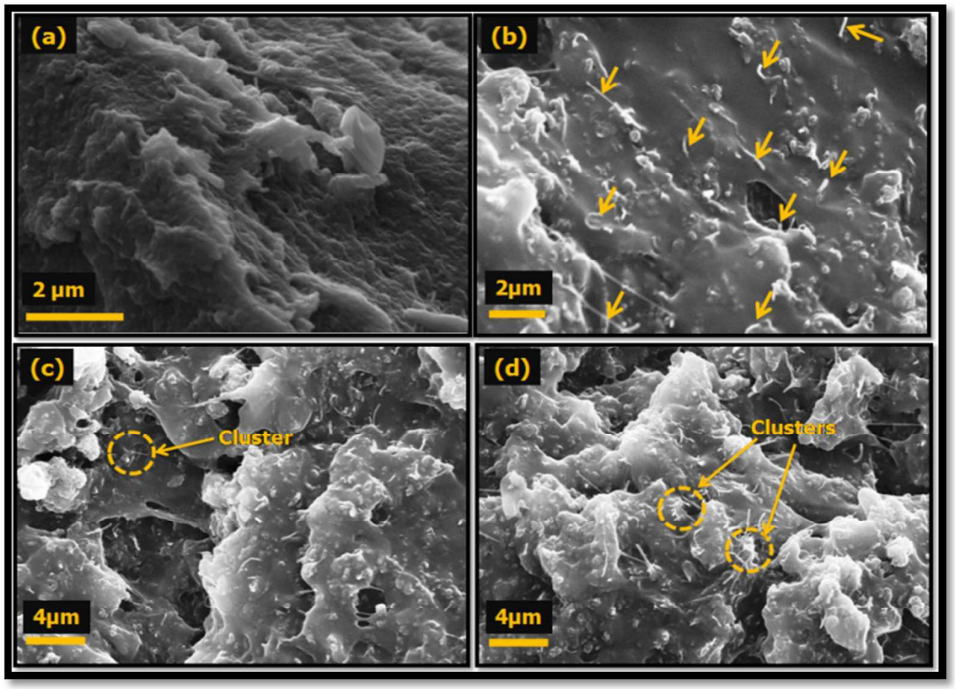


**Fig 3** SEM analyses of fractured surface of PU filled with PEDOT and PCNT filler (a) PUP3 film (b) PUPCNT1 showing uniform distribution of PCNT filler, (c) & (d) shows that PUPCNT2 and PUPCNT3 with excess loading of PCNT filler leads to clusters formation, respectively.

The fractured cross sectional surface of the composites was observed in the SEM. Fig 3 (a) shows fractured surface of PUP3, with indiscriminate distribution of PEDOT filler in the PU matrix. In Fig 3 (b) the fractured surface of PUPCNT1 with uniformly distributed PCNT filler in the PU matrix can be distinctly observed. The PCNT filler which appears as white bright lines embedded in PU matrix are marked with red arrows in the Fig 3 (b). The white bright lines increased with the increase of PCNT loading in the PU matrix (see Fig 3 c and d, respectively). It is interesting to note that PCNT filler exhibits good dispersion except one or two clusters in the PUPCNT2 and PUPCNT3 composite due to excessive loading. It is very well known that aggregation of the fillers in the matrix is responsible for poor mechanical properties. This supports the reason behind improved tensile strength of PUPCNT composites than pure PU.

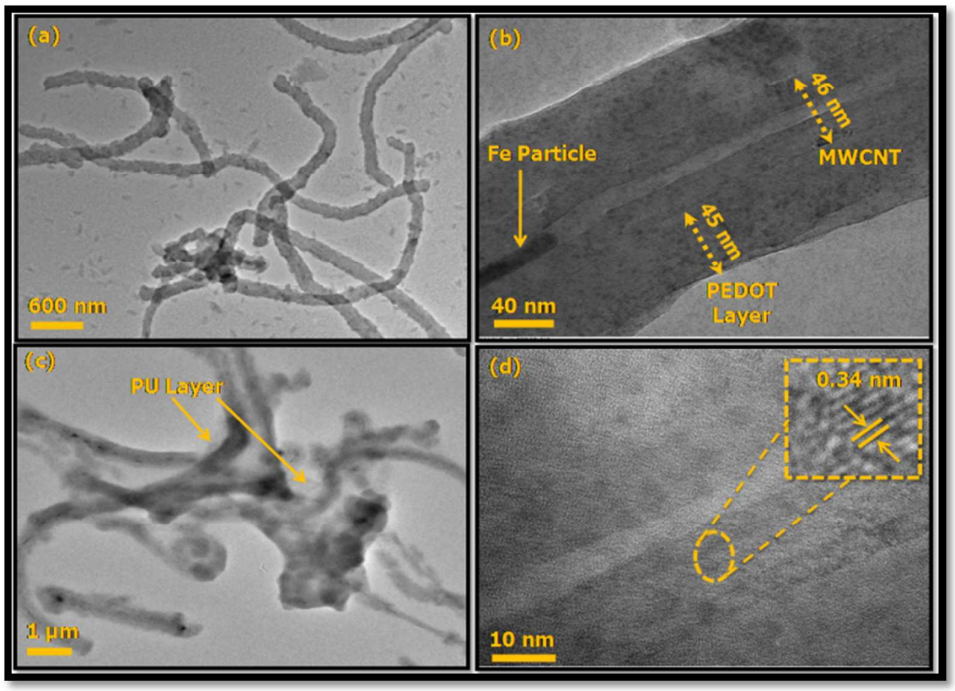


**Fig 4** TEM images (a) low magnification image of PCNT filler showing distinctly separated filler tubes, (b) high magnification image of PCNT showing thickness of PEDOT coating over MWCNT and presence of Fe catalyst inside MWCNTs (c) PUPCNT1 film image showing PCNT filler incorporated in PU matrix, and (d) HRTEM of PCNT filler showing spacing between adjacent layers of carbon nanotube walls

TEM images were further used to examine the core shell structure and thickness of PEDOT coating over MWCNTs. Fig 4 (a) shows the TEM image of PCNT filler where individual PCNTs can be clearly observed. Fig 4 (b) TEM image further confirms that MWCNTs are packed underneath the PEDOT layer. The diameter of PCNT filler and embedded MWCNT is about ~150 and ~46 nm, respectively, revealing thick coating of PEDOT layer (~45 nm). The presence of Fe particle can also be observed inside the MWCNTs which is remnant of ferrocene catalyst used during preparation of MWCNTs. Fig 4 (c) shows PCNT filler incorporated PU matrix where individually distributed PCNT filler can be clearly observed. Fig 4 (d) shows HRTEM image of PCNT filler with inset of the image showing spacing of 0.34 nm between the concentric carbon nanotubes in the PEDOT matrix.

**5.2 XRD**

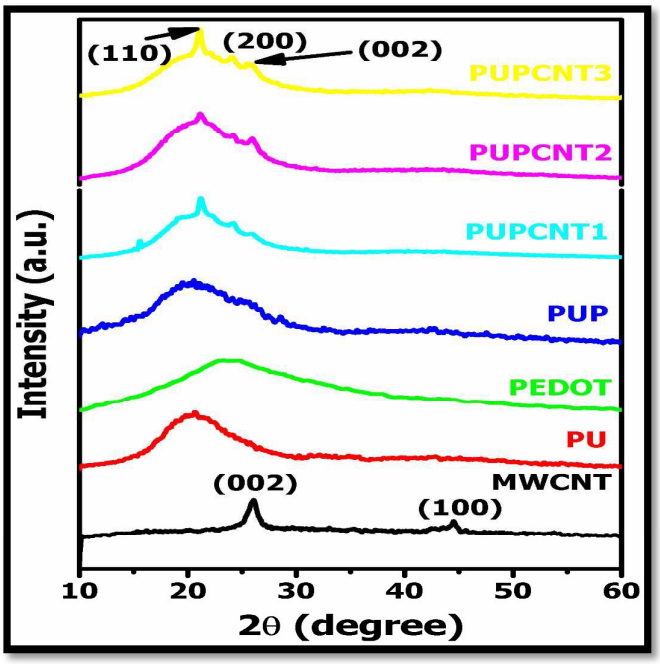


**Fig 5** XRD patterns of pristine MWCNT, PU, PEDOT, PUP, and PUPCNT composites

Fig 5 shows the XRD patterns of MWCNT, PU, PEDOT, PUP and PUPCNT composites. The XRD pattern of MWCNT shows two peak at 2θ value of 26.1° and 43.2° for (002) and (100) planes of carbon atoms. These peaks imply the interlayer spacing of 0.34 and 0.21 nm, respectively[24]. PU shows two peaks at 21.1° and 23.4° because of the crystals of polycaprolactone (PCL) corresponding to (110) and (200) planes[25]. A broad diffraction peak at 24.5° is observed for PEDOT, due to its amorphous nature. Since PEDOT does not show any significant peak the PUP presents a much broader peak than PEDOT and PU. In the PUPCNT composites the peaks of PCL and MWCNTs are present at their respective 2θ values. Hence, it further confirms the co-existence of PCNT in the PU matrix.

### 5.3 FTIR

The FTIR spectra of PU, PUP3 and PUPCNT3 recorded using ATR accessory is shown in Fig 6. All the three samples have characteristics peaks of PU. The characteristic peaks observed near 3320, and 1722 $cm^{-1}$ arises due to the stretching vibrations of $-NH$ and $-C=O$ groups in PU[26]. Other peaks observed in the PU spectrum are assigned in the table given

with Fig 6. The spectrum of PEDOT shows bands at 678, 829, 917, and 967 $cm^{-1}$ which are due to the deformation modes of $C-S-C$ in the thiophene ring; the peaks at 1052, 1084, 1134, and 1187 $cm^{-1}$ arises due to bending vibration of $C-O-C$ of ethylene group; the peaks at 1312 and 1512 $cm^{-1}$ corresponds to $C-C$ or $C=C$ stretching of quinoid structure and ring stretching of thiophene ring, respectively[27]. Inspite of some minor differences, PU, PUP3 and PUPCNT3 exhibits similar spectra due to the presence of significant amount of PU in matrix.

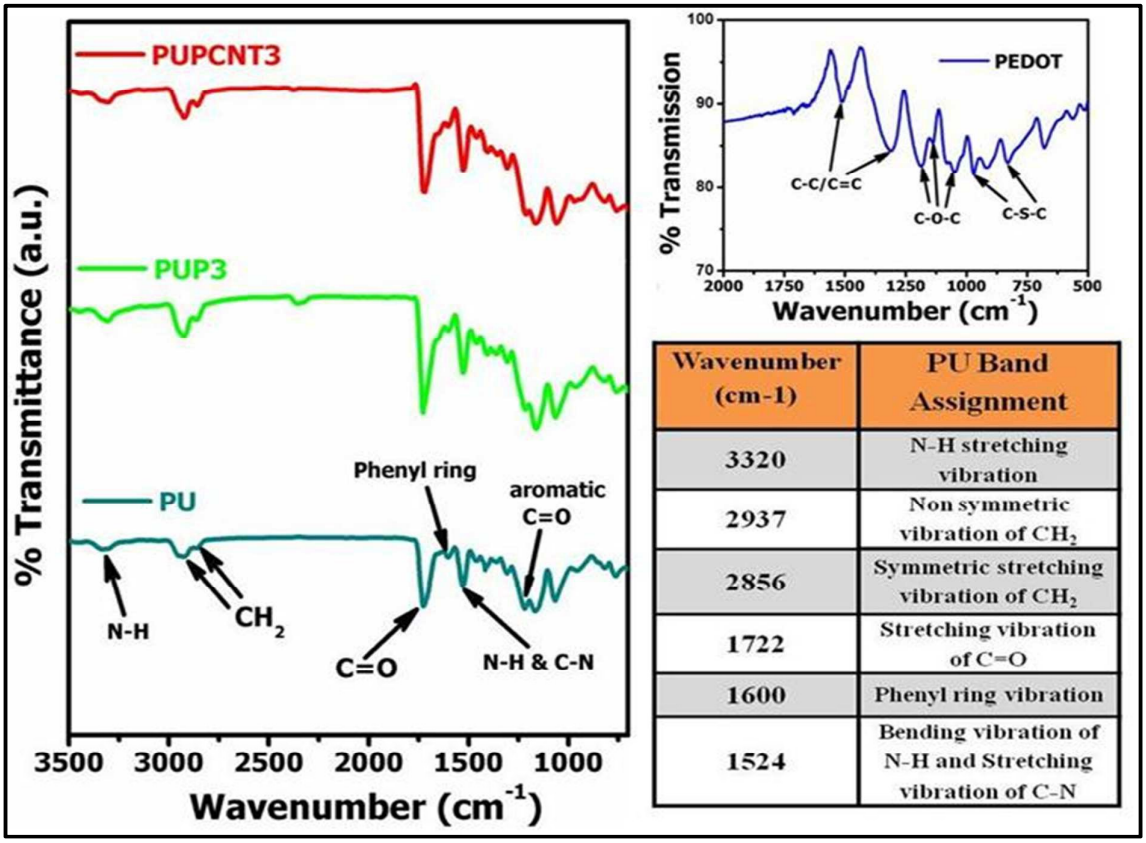


| Wavenumber (cm-1) | PU Band Assignment |
|---|---|
| 3320 | N-H stretching vibration |
| 2937 | Non symmetric vibration of $CH_2$ |
| 2856 | Symmetric stretching vibration of $CH_2$ |
| 1722 | Stretching vibration of C=O |
| 1600 | Phenyl ring vibration |
| 1524 | Bending vibration of N-H and Stretching vibration of C-N |

**Fig 6** FTIR spectra of PU, PUP3, PUPCNT3 and PEDOT samples with table assigning bands of PU

**Tensile Strength Test:**

Fig 7 shows the effect of filler loading on the tensile strength of PUP and PUPCNT composites. It is well known that pure conducting polymers are mechanically very weak. The blending of PEDOT filler in the PU matrix deteriorates the strength of PUP composites consistently. This can be attributed to the weak interaction between filler and matrix. It is striking to note that addition of 10 % PCNT filler, significantly increases the tensile strength

from 20 MPa to 26 MPa. This enhancement can be attributed to the homogeneous dispersion of PCNT and effective load transfer from the matrix to MWCNTs embedded in PEDOT. However, with further increase in PCNT loading to 20 and 30 wt%, the tensile strength decreases gradually decreases because of the plasticization effect on the mechanical properties, caused by the thick coating of PEDOT layer which has a very poor mechanical strength. Hence, tensile strength decreases with increasing loading of PCNT filler, since amount of PEDOT contributing to PCNT is greater than MWCNTs.

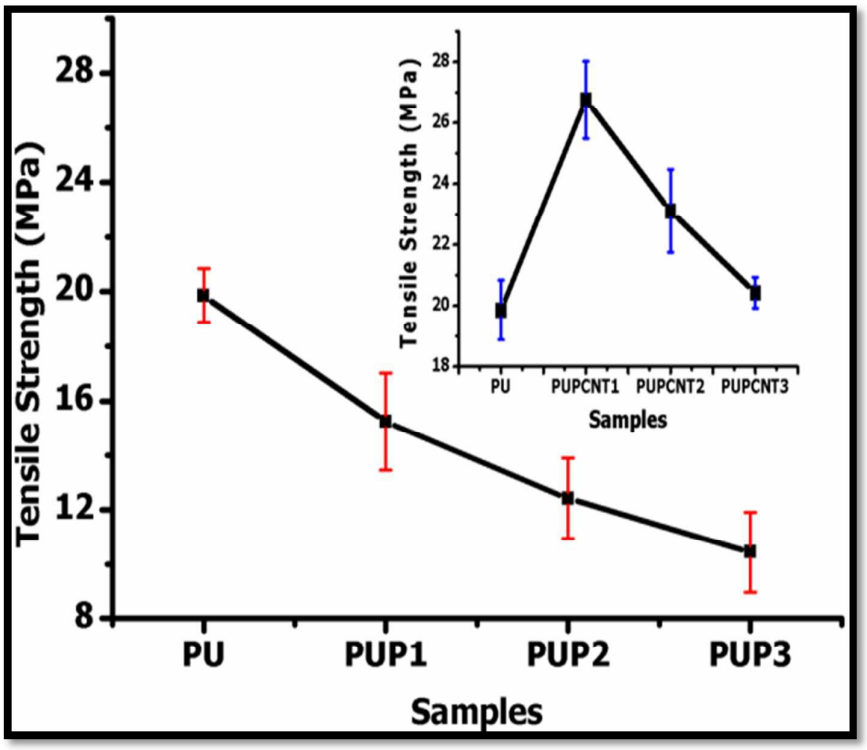


**Fig 7** Tensile strength of PU, PUP1, PUP2, and PUP3 while inset shows the tensile test of PU, PUPCNT1, PUPCNT2, and PUPCNT3

## 6 EMI shielding

The electromagnetic (EM) wave consists of two components; an electric field and a magnetic field, which are perpendicular to each other and change periodically. The EMI SE is described as the logarithmic ratio of transmitted power ($P_t$) to incident power ($P_i$) of radiation and is measured in dB. The mechanism of attenuation of EM wave by a shield depends on

three factors; (1) reflection, occuring at the surface of the shield; (2) absorption, which arises when EM wave travels inside the shield; and (3) multiple reflections of the EM wave at various interfaces (see fig 8 a). Therefore, the total EMI SE is the sum of the effectiveness of reflection ($SE_R$), absorption ($SE_A$) and multiple-reflections ($SE_M$) and can be expressed as[6,28]:

$$SE_T(dB) = SE_A + SE_R + SE_M = 10\log_{10}\left(\frac{P_t}{P_i}\right) \quad \textbf{Eq. 1}$$

$$SE_A = -\log\left(\frac{T}{1-R}\right) \quad \textbf{Eq. 2}$$

$$SE_R = -\log(1-R) \quad \textbf{Eq. 3}$$

where, R and T represents reflectance and transmittance, respectively.

$SE_M$ corresponds to the multiple reflections occurring at the various interfaces or surfaces within the shielding material. The absorption and reflection phenomenon directly effects the $SE_T$ on the other hand, multiple reflection decreases the overall SE. If the thickness of the shield is greater than skin depth (distance of the shield at which wave strength decreases to 1/e), the multiple reflection can be neglected. The skin depth (δ) is related to angular frequency (ω), relative permeability (μ') and ac conductivity ($\sigma_{ac}$) and can be expressed as $\delta = \sqrt{2/\omega\mu'\sigma_{ac}}$. According to electromagnetic theory, when the thickness of the shield is greater than the skin depth (t > δ), the frequency (ω) dependence of the far field losses can be expressed in terms of ac conductivity ($\sigma_{ac}$), real permeability (μ'), skin depth (δ), and thickness (t) of the shield material as[29-30]:

$$SE_R(dB) = 10\log\{\sigma_{ac}/16\omega\varepsilon_0\mu'\} \quad \textbf{Eq. 4}$$

$$SE_A(dB) = 20\{t/\delta\}\log e = 20\,t\sqrt{\mu\omega\sigma_{ac}/2}\log e = 8.68\{t/\delta\} \quad \textbf{Eq. 5}$$

The $\sigma_{ac}$ and δ are related to the imaginary permittivity (ε'') and real permeability (μ') as $\sigma_{ac} = \omega\varepsilon_0\varepsilon''$ and $\delta = \sqrt{2/\omega\mu'\sigma_{ac}}$ which gives absorption loss as:

$$SE_A(dB) = 8.68t\sqrt{\omega\mu'\sigma/2} \quad \textbf{Eq. 6}$$

It is known that $SE_A$ becomes more dominant as compared to the $SE_R$ in the microwave region. This is due to the shallow skin depth (δ) and high conductivity ($\sigma_{ac}$) values at such high frequencies. The $SE_T$ value for the PU, PUP and PUPCNT composites in the frequency range of 12.4-18 GHz is shown in Fig 8 (b). It is clearly visible from the Fig 8 (b) that PU

film sample gives negligible attenuation to EM waves whereas, the solution mixing of PEDOT polymer in the PU matrix gives 3.98 dB, 5.75 dB and 7.41 dB of attenuation at mid frequency of 15.2 GHz, for the composites; PUP1, PUP2 and PUP3, respectively. On the other hand, solution mixing of PCNT filler in the PU matrix, results in linear enhancement of the $SE_T$ of the PUPCNT composites. The maximum EMI SE obtained with PUPCNT3 was 44.25 dB at 15.2 GHz which is due to the formation of conducting networks throughout the electrically insulating PU matrix by the addition of PCNT filler having high aspect ratio. The EMI SE of electrically conductive polymer composites strongly depends upon conductivity, dispersion, aspect ratio and loading of conductive filler in the polymer matrix. To investigate the shielding mechanism, the total shielding effectiveness is further resolved into reflection loss ($SE_R$) and absorption loss ($SE_A$) components as shown in Fig 8 (c) and (d). From the experimental measurements, it is observed that the SE due to absorption and reflection ($SE_A$ and $SE_R$) increases with increasing loading of the fillers (PEDOT and PCNT). This can be attributed to the increase in conductivity of the composites. It is interesting to note that the contribution of $SE_A$ for the attenuation of EM wave is greater than the $SE_R$, due to increase in conductivity, dielectric losses as well as magnetic permeability (entrapped Fe catalyst particles in the MWCNTs). Fig 8 (c) shows an anomalous behaviour of $SE_R$ of the samples in the applied frequency range. The $SE_R$ of PU is almost constant throughout the frequency range due to its insulating nature, whereas $SE_R$ of PUP3 and PUPCNT1 increases with frequency. It is because the samples with loading of 30% of PEDOT and 10% of PCNT in PU matrix, respectively, were able to reach the percolation threshold (formation of continuous electrically conducting network in the matrix) with uniform conductivity. The decrease in $SE_R$ of PUP1 and PUP2 with increase in frequency can be attributed to the inability of PEDOT filler with 10% and 20% loading in PU matrix respectively to form the electrically conducting path whereas in case of PUPCNT2 and PUPCNT3 the decrease in $SE_R$ is because of cluster formation due to excessive loading of PCNT filler in the PU matrix which causes heterogeneity at the nano-level (non uniform conductive network) thereby resulting in decreased $SE_R$ values. The total shielding effectiveness of PUPCNT is greater than PUP composites and it increases systematically with increasing loading of PCNT.

We have also correlated various shielding parameters of the material with the ac conductivity while attenuation constant was measured to determine the attenuation properties of the material.

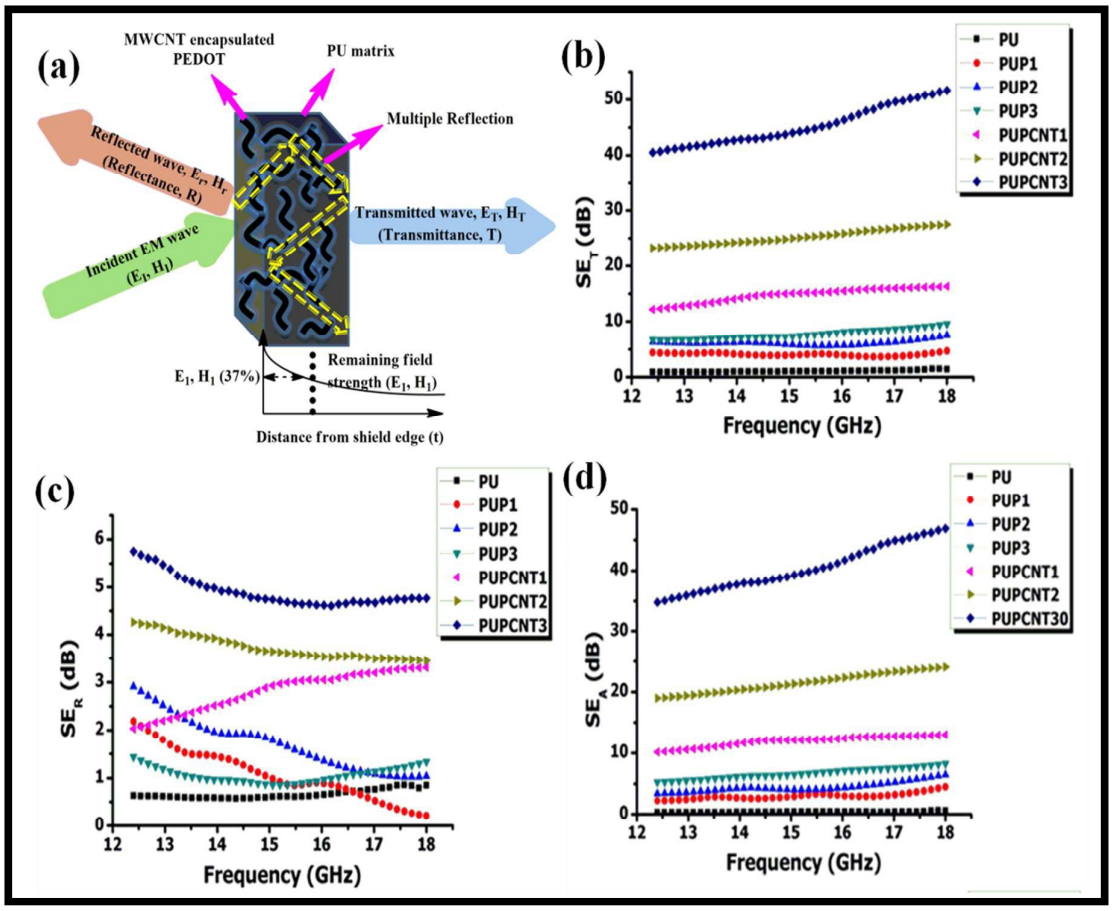


**Fig 8 (a)** Basic mechanism of EMI shielding by PUPCNT composite, (b) Frequency dependence of total shielding effectiveness ($SE_T$), (c) losses due to reflection ($SE_R$) and (d) absorption ($SE_A$) of different samples of PU composites

### 6.1 Electrical conductivity and EMI shielding

The variation in electrical conductivity and EMI SE (at 12.4 GHz) of PU, PUP, and PUPCNT composites at room temperature is shown in Fig 9. The electrical conductivity of neat PU is $1.53\times 10^{-11}$ S/cm. The loading of PEDOT (10, 20, and 30 wt%) in PU matrix slightly increases the conductivity by 3-4 orders of magnitude. On the other hand loading of 10 wt% PCNT filler increases the conductivity of composite by the orders of 7-8 magnitude. This indicates the formation of electrical percolation threshold in the PU matrix. The electrical conductivity of the PUPCNT composites increases with filler loading and the value reaches upto 2.7 S/cm from $1.53 \times 10^{-11}$ S/cm of pure PU. This is due to the high aspect ratio of

PCNT filler which helps in establishing it an excellent conductive network between PU and PCNT. The SEM images of fractured PUPCNT composites showing good dispersion of the filler in the PU matrix, further confirms the formation of conductive network throughout the matrix. It is a well know fact that the increase in electrical conductivity enhances the EMI shielding values of the composites (see Table 2) and is clearly depicted in the fig 9.

**Table 2** Variation of EMI SE (dB) of PU composites with room temperature Electrical conductivity at 12.4 GHz

| **SI No.** | **Sample** | **Conductivity (S/cm)** | **$SE_T$ (dB)** |
|---|---|---|---|
| 1 | PU | $1.53 \times 10^{-11}$ | 0.9353 |
| 2 | PUP1 | $5.8 \times 10^{-8}$ | 4.396 |
| 3 | PUP2 | $4.83 \times 10^{-8}$ | 6.322 |
| 4 | PUP3 | $4.36 \times 10^{-7}$ | 6.667 |
| 5 | PUPCNT1 | $2.75 \times 10^{-4}$ | 12.204 |
| 6 | PUPCNT2 | $3.06 \times 10^{-1}$ | 23.232 |
| 7 | PUPCNT3 | 2.7 | 40.535 |

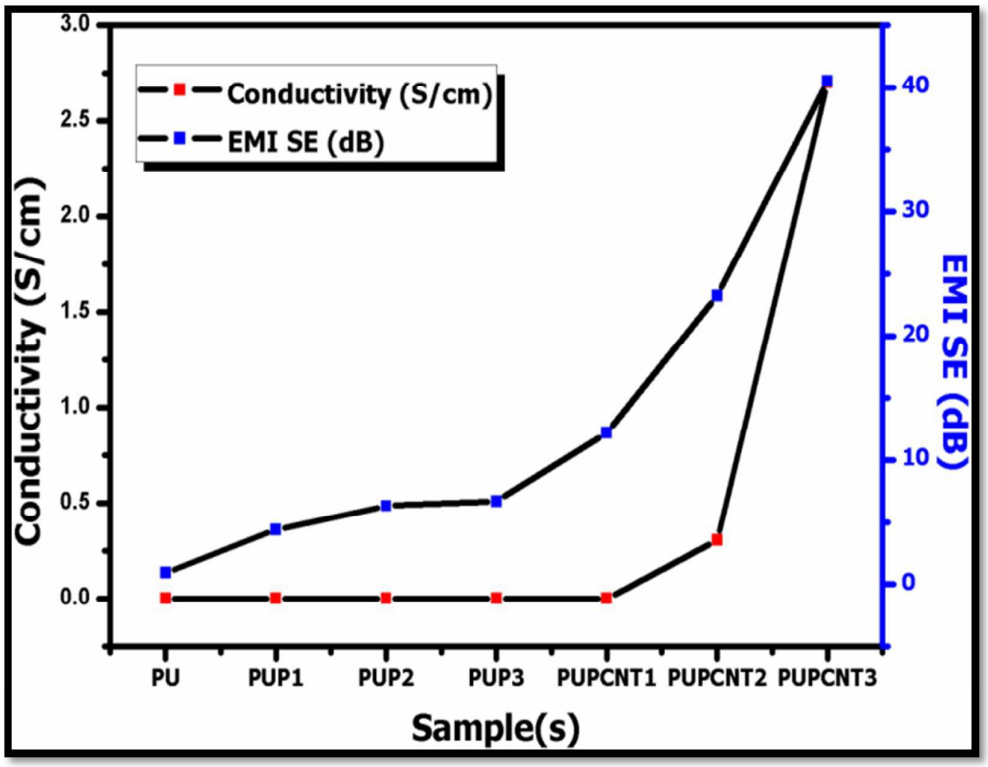


**Fig 9** Variation of EMI SE (dB) with increase in room temperature dc electrical conductivity of different samples

### 6.2 Electromagnetic attributes

To investigate the observed values of SE, the electromagnetic attributes i.e. complex permittivity ($\varepsilon' - j\varepsilon''$) and permeability ($\mu' - j\mu''$) were measured. These parameters were calculated from experimental scattering parameters ($S_{11}$ and $S_{22}$) using theoretical calculations given in Nicolson-Ross-Weir algorithm[31]. It is known that, the $\varepsilon'$ and $\varepsilon''$ of the electromagnetic attributes is due to the amount of polarization occurring in the material. The dielectric values of the material depend on its ionic, electronic, orientation (arising due to the presence of bound charges) and space charge polarization (due to the heterogeneity in the system). In addition, interfacial polarization (also known as Maxwell-Wagner polarization[32]) due to different dielectric constants and conductivities of the individual components in the heterogeneous system further enhances the electromagnetic attributes. In case of PUPCNT composites, PEDOT coated MWCNTs were incorporated in the PU matrix having different dielectric constants and conductivities and hence show interfacial polarization in the applied frequency range. The presence of conductive filler PCNT in the insulating PU matrix leads to the formation of various interfaces and a heterogeneous system, the space charge

accumulating at these interfaces results in the higher microwave absorption[33]. ICP's consists of polaron (radical cation) and bipolaron (biradical cation) which are free to move along the polymer backbone. ICP's also possess bound charges (dipoles) which have restricted mobility leading to strong polarization in the material. Hence, orientation and dipolar polarization is probably contributed to the dielectric permittivity. Fig 10 shows dielectric constants and dielectric losses of PU, PUP3, and PUPCNT3 composites in the 12.4-18 GHz frequency range. It is observed that PUPCNT3 have higher values of dielectric loss and dielectric constant (ε' ~ 26.08 - 23.5 and ε'' ~ 17.75 – 12.9) than PUP3 ( ε' ~ 6.5 – 6.24 and ε'' ~ 2.06 – 1.82) which are much higher than in-comparison to neat PU ( ε' ~ 2.21 – 2.04 and ε'' ~ 0.41 – 0.32). The synergistic effect of PCNT filler in the PU matrix leads to the increased amount of polarization which contributes to the high dielectric attributes of the PUPCNT3 composites.

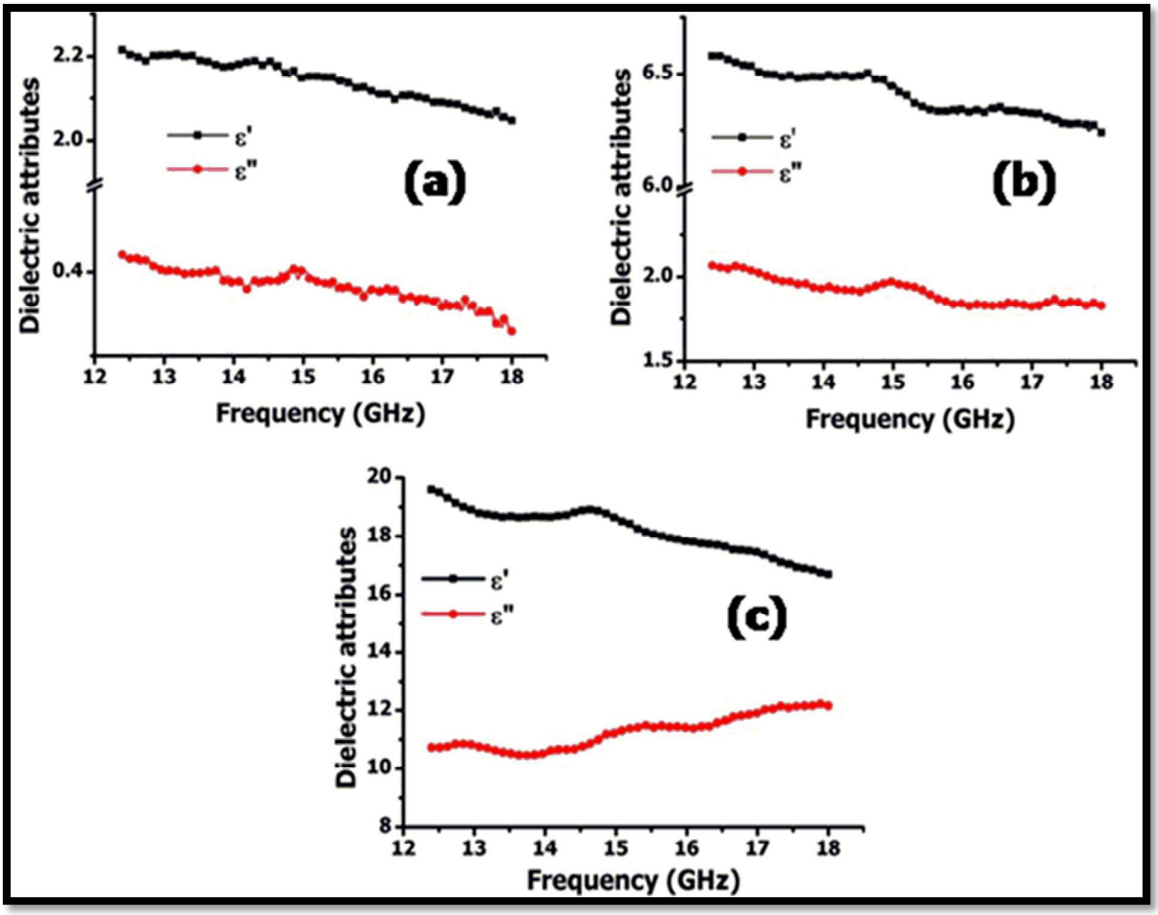

**Fig 10** Behaviour of dielectric constant (ε') and dielectric loss (ε'') of PU (a), PUP3 (b), PUPCNT (c) samples as function of frequency

**Table 3** EMI shielding performance of different conductive polymer composites containing CNTs as conducting filler

| Matrix | Filler | Concentration | Frequency | $SE_T$ (dB) | Reference |
|---|---|---|---|---|---|
| PU | f-MWCNTs | 10 wt% | X-band | ~29 | [19] |
| PU | SWCNTs | 20 wt% | X-band | 17 | [34] |
| PU | $TiO_2$ coated MWCNT | 15 wt % | 10.98 GHz | 42.53 | [22] |
| PU | MWCNT | 22 wt% | X-band | 20 | [20] |
| PU | MWCNT | 10 wt% | X-band | 41.6 | [35] |
| TPU | MWCNT | 10 wt% | X-band | 22 | [21] |
| SCPU | MWCNT | 5 wt% | 8.8 GHz | 22 | [36] |
| PMMA | MWCNT | 40 wt% | 50 MHz-13.5 GHz | 27 | [37] |
| PMMA | MWCNT | 10 vol% | X-band | 40 | [38] |
| Epoxy | SWCNT | 15 wt% | 500 MHz-1.5 GHz | 15-20 | [39] |
| Epoxy | SWCNT | 15 wt% | X-band | 20-30 | [40] |
| PC | MWCNT | 15 wt% | X-band | 27 | [41] |
| PVA | MWCNT | 10 wt% | 8 GHz | 15 | [42] |
| EMA | MWCNT | 10 wt% | X-band | ~20 | [43] |
| PTT | MWCNT | 10 wt% | Ku-band | 42 | [44] |
| PU | PEDOT coated MWCNT | 30 wt% | 12.4 GHz | 45 | This work |

**Electrostatic Dissipation studies:**

ESD is critical for highly sensitive electronics and industrial applications. An electrostatic dissipative material prevents the unwanted charge build-up that could otherwise transfer to sensitive electronic components. It helps in grounding of potentially hazardous charges. For ESD, typically a surface resistivity of $10^6$-$10^9$ Ω $sq^{-1}$ is required. The room temperature DC conductivity test of samples showed that PUP composites can be effectively used for ESD applications. Since PUP composites failed to reach the minimum EMI SE (20 dB) required for most commercial applications in EMI measurements. We carried out ESD measurements of PUP composites by JCI 155v5 charge decay test unit. Fig 12 shows the static decay time of PUP1, PUP2 and PUP3 samples measured by applying a positive voltage of 5000 V. From the measurements it is observed that PUP1, PUP2 and PUP3 composites shows a decay time of less than 0.2 second for the initial peak voltage to reach 1/e (about 37%) which meets the required time limit less than half a second in the 1/e criterion. We also measured the 10% criterion (initial peak voltage to 10% within 2 seconds) and it is observed that all the samples show an excellent 10 % criterion decay time of less than 0.8 second. Hence, ESD results indicate that loading of PEDOT in PU increases the conductivity of composites required for static charge dissipation. Thus, it is better to use PUP composites for ESD rather than EMI shielding applications.

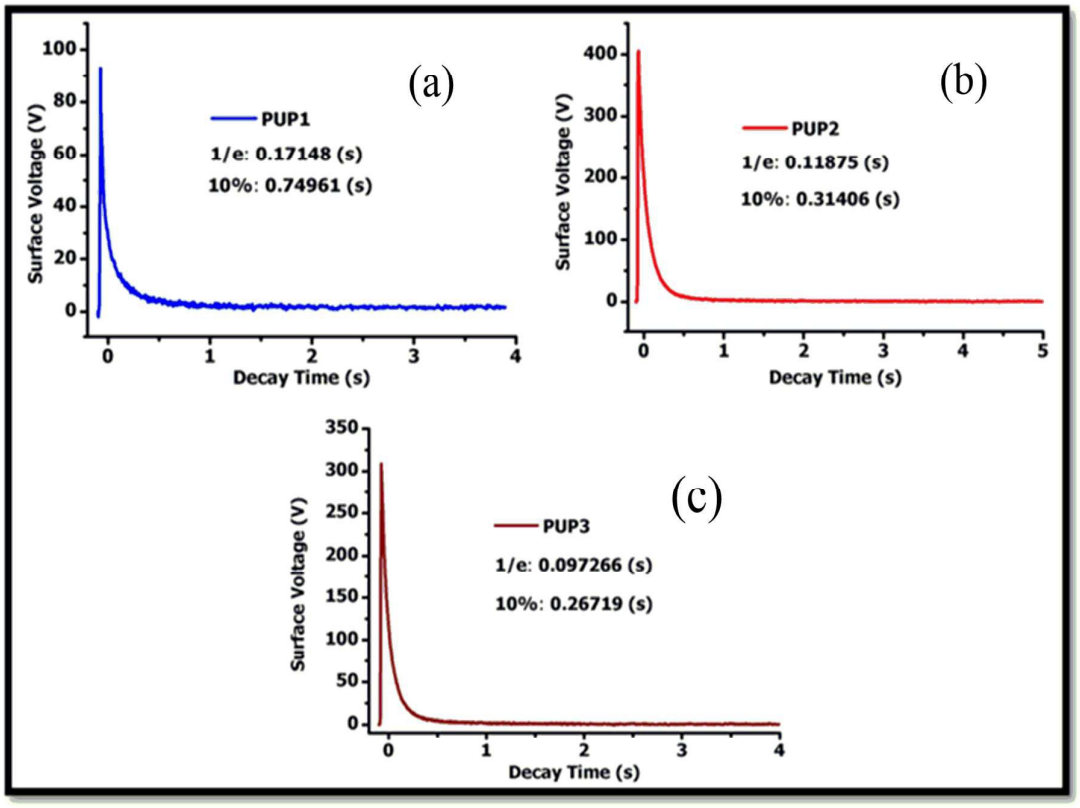

**Fig 3** Static charge decay time of (a) PUP1, (b) PUP2, and (c) PUP3 samples at charging voltage of 5.0 kV

## 7 Conclusion

Specially designed sandwich composites were prepared by blending PEDOT modified MWCNTs in PU matrix by solution casting. The composites showed improved mechanical, electrical and EMI SE properties. The PEDOT grafted MWCNTs exhibit enhanced dispersion in the PU matrix which results in improved tensile strength of the composites with 10 and 20 wt% loading of the filler. Moreover, the EMI SE of the PUPCNT composites increases significantly on increasing filler's loading due to the formation of enhanced conductive network in the PU matrix. The maximum SE of 45 dB was observed with 30 wt% loading of PCNT filler in the PU matrix which is the highest as compared to other CNT composites made for EMI shielding applications. The absorption dominated shielding mechanism was observed. Hence, EMI shielding results suggest that these brand new flexible conducting materials can effectively be used as next generation shielding materials.

## Acknowledgements

The authors are grateful to the Director CSIR-National Physical Laboratory, New Delhi for his kind support and encouragement. The authors also wish to thank Mr. K. N. Sood, Mr Dinesh Singh and Mrs Shweta Sharma for the SEM, TEM and tensile strength characterizations, respectively.

## References

(1) Tzeng, S.-S.; Chang, F.-Y. *Materials Science and Engineering: A* **2001**, *302*, 258.
(2) Han, E. G.; Kim, E. A.; Oh, K. W. *Synthetic Metals* **2001**, *123*, 469.
(3) Chung, D. D.; Shui, X.; Google Patents: 1998.
(4) Huang, C.-Y.; Mo, W.-W.; Roan, M.-L. *Surface and Coatings Technology* **2004**, *184*, 163.
(5) Chung, D. D. L. *Carbon* **2001**, *39*, 279.
(6) Wang, Y.; Jing, X. *Polymers for Advanced Technologies* **2005**, *16*, 344.
(7) Kim, Y. H.; Sachse, C.; Machala, M. L.; May, C.; Müller-Meskamp, L.; Leo, K. *Advanced Functional Materials* **2011**, *21*, 1076.
(8) Pozo-Gonzalo, C.; Mecerreyes, D.; Pomposo, J. A.; Salsamendi, M.; Marcilla, R.; Grande, H.; Vergaz, R.; Barrios, D.; Sánchez-Pena, J. M. *Solar energy materials and solar cells* **2008**, *92*, 101.
(9) Van Dijken, A.; Perro, A.; Meulenkamp, E.; Brunner, K. *Organic Electronics* **2003**, *4*, 131.

(10) Qiu, C.; Wang, J.; Mao, S.; Guo, W.; Cheng, S.; Wang, Y. *Polymers for Advanced Technologies* **2010**, *21*, 651.

(11) Gopalan, A. I.; Lee, K.-P.; Santhosh, P.; Kim, K. S.; Nho, Y. C. *Composites Science and Technology* **2007**, *67*, 900.

(12) Zhang, X.; Zhang, J.; Wang, R.; Zhu, T.; Liu, Z. *ChemPhysChem* **2004**, *5*, 998.

(13) Deng, J.; Ding, X.; Zhang, W.; Peng, Y.; Wang, J.; Long, X.; Li, P.; Chan, A. S. C. *European Polymer Journal* **2002**, *38*, 2497.

(14) Cheng, J.; Zhao, B.; Zheng, S.; Yang, J.; Zhang, D.; Cao, M. *Applied Physics A* **2015**, *119*, 379.

(15) Kotsilkova, R.; Ivanov, E.; Bychanok, D.; Paddubskaya, A.; Demidenko, M.; Macutkevic, J.; Maksimenko, S.; Kuzhir, P. *Composites Science and Technology* **2015**, *106*, 85.

(16) Al-Saleh, M. H. *Synthetic Metals* **2015**, *205*, 78.

(17) Verma, P.; Saini, P.; Malik, R. S.; Choudhary, V. *Carbon* **2015**, *89*, 308.

(18) Chen, M.; Zhang, L.; Duan, S.; Jing, S.; Jiang, H.; Luo, M.; Li, C. *Nanoscale* **2014**, *6*, 3796.

(19) Gupta, T. K.; Singh, B. P.; Dhakate, S. R.; Singh, V. N.; Mathur, R. B. *Journal of Materials Chemistry A* **2013**, *1*, 9138.

(20) Hoang, A. S. *Advances in Natural Sciences: Nanoscience and Nanotechnology* **2011**, *2*, 025007.

(21) Ramôa, S. D. A. S.; Barra, G. M. O.; Oliveira, R. V. B.; de Oliveira, M. G.; Cossa, M.; Soares, B. G. *Polymer International* **2013**, *62*, 1477.

(22) Bhattacharya, P.; Sahoo, S.; Das, C. *Exp Polym Lett* **2013**, *7*, 212.

(23) Mathur, R. B.; Chatterjee, S.; Singh, B. P. *Composites Science and Technology* **2008**, *68*, 1608.

(24) Cao, A.; Xu, C.; Liang, J.; Wu, D.; Wei, B. *Chemical Physics Letters* **2001**, *344*, 13.

(25) Ajili, S. H.; Ebrahimi, N. G. In *Macromolecular symposia*; Wiley Online Library: 2007; Vol. 249, p 623.

(26) Zhang, X.; Xu, R.; Wu, Z.; Zhou, C. *Polymer International* **2003**, *52*, 790.

(27) Zhou, W.; Hu, X.; Bai, X.; Zhou, S.; Sun, C.; Yan, J.; Chen, P. *ACS Applied Materials & Interfaces* **2011**, *3*, 3839.

(28) Colaneri, N. F.; Schacklette, L. *Instrumentation and Measurement, IEEE Transactions on* **1992**, *41*, 291.

(29) Das, N.; Khastgir, D.; Chaki, T.; Chakraborty, A. *Composites part A: applied science and manufacturing* **2000**, *31*, 1069.

(30) Makeiff, D. A.; Huber, T. *Synthetic Metals* **2006**, *156*, 497.

(31) Baker-Jarvis, J. J.; Grosvenor, M. *Transmission/Reflection and Short-Circuit Line Methods for Measuring Permittivity and Permeability*.

(32) Zhu, J.; Gu, H.; Luo, Z.; Haldolaarachige, N.; Young, D. P.; Wei, S.; Guo, Z. *Langmuir* **2012**, *28*, 10246.

(33) Singh, K.; Ohlan, A.; Pham, V. H.; Balasubramaniyan, R.; Varshney, S.; Jang, J.; Hur, S. H.; Choi, W. M.; Kumar, M.; Dhawan, S. *Nanoscale* **2013**, *5*, 2411.

(34) Liu, Z.; Bai, G.; Huang, Y.; Ma, Y.; Du, F.; Li, F.; Guo, T.; Chen, Y. *Carbon* **2007**, *45*, 821.

(35) Gupta, T. K.; Singh, B. P.; Teotia, S.; Katyal, V.; Dhakate, S. R.; Mathur, R. B. *J Polym Res* **2013**, *20*, 1.

(36) Liu, Z.; Bai, G.; Huang, Y.; Li, F.; Ma, Y.; Guo, T.; He, X.; Lin, X.; Gao, H.; Chen, Y. *The Journal of Physical Chemistry C* **2007**, *111*, 13696.

(37) Kim, H. M.; Kim, K.; Lee, C. Y.; Joo, J.; Cho, S. J.; Yoon, H. S.; Pejaković, D. A.; Yoo, J. W.; Epstein, A. J. *Applied Physics Letters* **2004**, *84*, 589.

(38) Pande, S.; Singh, B. P.; Mathur, R. B.; Dhami, T. L.; Saini, P.; Dhawan, S. K. *Nanoscale Res Lett* **2009**, *4*, 327.

(39) Li, N.; Huang, Y.; Du, F.; He, X.; Lin, X.; Gao, H.; Ma, Y.; Li, F.; Chen, Y.; Eklund, P. C. *Nano Letters* **2006**, *6*, 1141.

(40) Huang, Y.; Li, N.; Ma, Y.; Du, F.; Li, F.; He, X.; Lin, X.; Gao, H.; Chen, Y. *Carbon* **2007**, *45*, 1614.

(41) Singh, A. P.; Gupta, B. K.; Mishra, M.; Govind; Chandra, A.; Mathur, R. B.; Dhawan, S. K. *Carbon* **2013**, *56*, 86.

(42) Salimbeygi, G.; Nasouri, K.; Shoushtari, A. M.; Malek, R.; Mazaheri, F. *Micro & Nano Letters, IET* **2013**, *8*, 455.

(43) Basuli, U.; Chattopadhyay, S.; Nah, C.; Chaki, T. K. *Polymer Composites* **2012**, *33*, 897.

(44) Gupta, A.; Choudhary, V. *Composites Science and Technology* **2011**, *71*, 1563.

## Graphical Abstract

**Sandwich composites of polyurethane reinforced with poly (3, 4-ethylene dioxythiophene) coated multiwalled carbon nanotubes with exceptional electromagnetic interference shielding properties**

**M. Farukh[ab], Ridham Dhawan[a], Bhanu P. Singh[c] and S.K.Dhawan[a*]**

Poly (3, 4-ethylene dioxythiophene)/MWCNT/PU composite films were designed which shows a shielding effectiveness of ~ 45 DB in the Ku-band and a static decay time of 0.2 sec which can find practical applications for control of electromagnetic pollution as well as antistatic material for encapsulation of electronic equipments.